Письма в ЭЧАЯ. 2014. Т. 11, № 5(189). С. 986–993

DEFLECTING RF STRUCTURES WITH REDUCED LEVEL OF ABERRATIONS FOR TRANSFORMATION OF PARTICLE DISTRIBUTIONS IN THE BUNCH

V. Paramonov [a, 1], *K. Floettmann* [b], *L. Kravchuk* [a], *P. Orlov* [a]

[a] Institute for Nuclear Research of the RAS, Moscow

[b] Deutsches Elektronen-Synchrotron ein Forschungszentrum der Helmholtz-Gemeinschaft, Hamburg, Germany

Deflecting RF structures find applications for the rotation of a bunch of charged particles. Their application for transformation of the particle distributions in the bunch results in additional requirements on the quality of the field distribution, i.e., the minimization of aberrations. Referring to the previous methodical analysis, deflecting structures with a reduced level of aberrations are developed both for traveling wave and standing wave operation. The application of such structures results in an essentially smaller emittance deterioration during bunch rotation.

Отклоняющие ВЧ-структуры находят применение для вращения сгустка заряженных частиц. Их применение для преобразования распределения частиц в сгустке приводит к дополнительным требованиям на качество распределения поля, минимизации аберраций. На основании проведенного методического анализа предложены отклоняющие структуры с пониженным уровнем аберраций как для режима бегущих, так и стоячих волн. Применение таких структур приводит к существенно меньшему искажению эмиттанса при вращении сгустка.

PACS: 06.60.-c

INTRODUCTION

In modern facilities with short and bright bunches Deflecting RF Structures (DS) find applications, such as short-bunch rotation for special diagnostics, emittance exchange experiments and luminosity enhancement in colliders. All these applications are related to the Transformation of the Particle Distributions (TPD) in the six-dimensional phase space. For TPD the DS operates in a different mode as compared to the bunch deflection. The applications for TPD result in additional specific requirements. Together with the expected transformations the DS introduces distortions due to particularities in the E_d distribution. The origin of the distortions is aberrations, generated by nonlinear additions in the field distribution, which are caused by higher spatial harmonics and other reasons, which need to be minimized because the tool for TPD should provide as minimal as possible intrinsic distortions.

[1] E-mail: paramono@inr.ru

1. FIELD ANALYSIS AND ABERRATIONS REDUCTION

For the description of the transverse deflecting field E_d a basis of hybrid waves HE_n–HM_n was introduced [1]. The common representation for the field distribution in the DS aperture is

$$\mathbf{E} = A\mathbf{E}_{HE_1} + B\mathbf{E}_{HM_1}, \tag{1}$$

where the weighting coefficients A, B depend both on the supporting structure and the operation mode. In the relativistic case $\beta = 1$, the main spatial harmonics of the deflecting field, both for HE_1 and HM_1 waves [1], are free from aberrations. For the Disk Loaded Waveguide (DLW) the well-known expressions for the field components were obtained in the small-pitch approximation [1], which neglects all higher spatial harmonics, $\beta = \beta_p = 1$, $d \ll \lambda$, $t_d \ll d$, where t_d is the disk thickness. The period length $d = \dfrac{\theta\beta\lambda}{2\pi}$ is defined from the synchronism with the main harmonic a_{j0}, where θ and λ are the operating phase advance and wavelength. The total deflecting field consists not only of the main spatial harmonics. A more detailed general analysis [2] of the field distribution near the axis revealed three reasons for nonlinear additions in periodical DS.

The first addition arises only in DS with a period length matched to the particle velocity $\beta = \beta_p < 1$. In the nonrelativistic case, already the field of the main harmonics is not free of nonlinear additions. The aberrations are important for low particle energy and vanish with $1/(\beta^2\gamma^2)$ for higher energies.

The second addition is the main source for transverse nonlinearities and arises from higher spatial harmonics. The effective deflecting field of the pth harmonic is

$$\begin{aligned} e_{dxp} &\approx \frac{k_{sp}\,(a_p + b_p)}{2}\left(1 + k_{sp}^2\frac{x^2+y^2}{4}\right)e_{zp}, \\ e_{dyp} &\approx \frac{k_{sp}\,(a_p + b_p)}{2}\left(k_{sp}^4(x^3y + y^3x)\right)e_{zp}, \\ k_{zp} &= \frac{k(\theta_0 + 2\pi p)}{\beta_z\theta_0}, \quad k_{sp}^2 = |k_{zp}^2 - k^2|, \end{aligned} \tag{2}$$

where e_{zp} is the corresponding harmonic of the E_z component.

The third addition arises due to a break of the rotational symmetry of DS, which is either a feature of the original DS design or which needs to be introduced in order to define the direction of the deflecting field. The nearest component has a sextupole wave structure, and the transverse force even of the main harmonic is nonlinear.

There is a large variety of RF structures with transverse fields, which can be used to deflect a bunch. In Fig. 1, a possible line of geometrical transformations of DS is shown. Despite a more or less continuous appearing transformation of geometries, the structures in Fig. 1, *a*, *b* and *d*, *e* have a quite different quality of the E_d distribution.

The main attention has been paid to the reduction of higher spatial harmonics in the deflecting field of the dipole mode. For each harmonic the transverse and the longitudinal distributions are rigidly coupled and are proportional to the harmonic amplitude a_{jp}. Spatial harmonics are essential at the aperture radius $r = a$ and higher harmonics attenuate toward

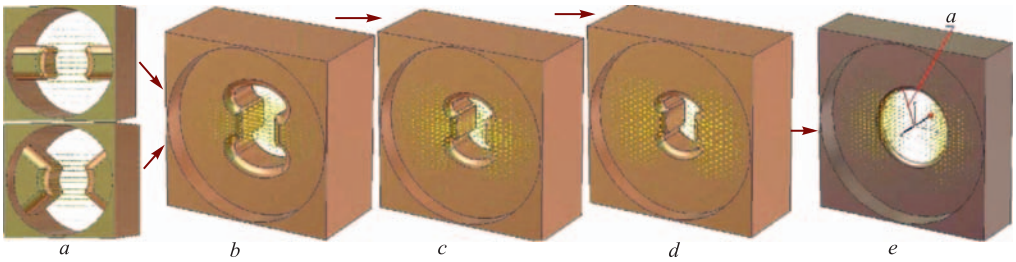

Fig. 1. Possible DS transformation

the axis as

$$a_{jp}(0) \sim a_{jp}(a)\,\exp\left(-\frac{4\pi^2 p}{\beta\theta}\,\frac{a}{\lambda}\right), \quad |p| \gg 1. \tag{3}$$

To estimate the harmonics individually and «in total», let us introduce the parameters $\delta\psi_j(z)$ and Ψ_j at the axis $0 \leqslant z \leqslant d$, $r = 0$,

$$\delta\psi_j(z) = \psi_j(z) + \frac{\theta z}{d}, \quad \Psi_j = \max\left(|\delta\psi_j(z)|\right), \tag{4}$$

with the physical sense as deviation and maximal deviation of the phase of the real wave component from the phase of the synchronous harmonic [2]. The value Ψ_d depends on the DS design and operating phase advance θ.

1.1. Traveling Wave Operation. The attenuation of higher spatial harmonics (3) is common for all periodical structures, and nonlinear additions in the deflecting field are hence reduced in DS with large apertures, operating in the Traveling Wave (TW) mode with $\theta \ll 180^\circ$. More important is the mutual phasing of the hybrid waves HE_1 and HM_1. The contribution of the pth harmonic in E_d vanishes (2) if $a_p \sim -b_p$, regardless of the amplitude of the corresponding harmonic e_{zp} in the original field. For opposite phasing of the hybrid waves HE_1 and HM_1, i.e., $A \cdot B < 0$, the higher spatial harmonic of the electric field E_x partially compensates the corresponding harmonic of the magnetic field H_y, while for equal phasing $A \cdot B > 0$, the amplitude of the deflecting force of the pth harmonic is even larger than the amplitudes for the field components.

The DLW structure in the first passband features an opposite phasing of the hybrid waves, and one can see in Fig. 2, *a* the slower rising of $\Psi_d(a, \theta)$ with θ, as compared to the corresponding rising $\Psi_z(a, \theta)$. Also, a clear canyon appears in the $\Psi_d(a, \theta)$ surface, corresponding to the condition $A \sim -B$. The TE structure [4], Fig. 1, *b*, features an equal phasing of the hybrid waves, and one can see in Fig. 2, *c* the faster rising of $\Psi_d(a, \theta)$ with θ, as compared to the corresponding rising $\Psi_z(a, \theta)$ and the absence of a canyon in the $\Psi_d(a, \theta)$ surface.

In Fig. 3, *a*, the plots of E_d and E_z distributions for a DLW in the TW mode with $\theta = 120^\circ$, which is similar to the well-known LOLA structure [3], are shown. The ripple in the distributions is caused by the higher spatial harmonics. Similar plots are shown in Fig. 3, *b* for a DLW with $\theta = 60^\circ$ and more balanced ratio of the hybrid waves. According to simulations with CST Micro Wave Studio, the higher spatial harmonics for the $\theta = 60^\circ$ structure are reduced ~ 40 times in E_z and ~ 3.5 times in E_d. At present, the DLW structure in the TW mode with $\theta \sim 60^\circ$ represents the optimum in the field distribution quality for the six-dimensional TPD.

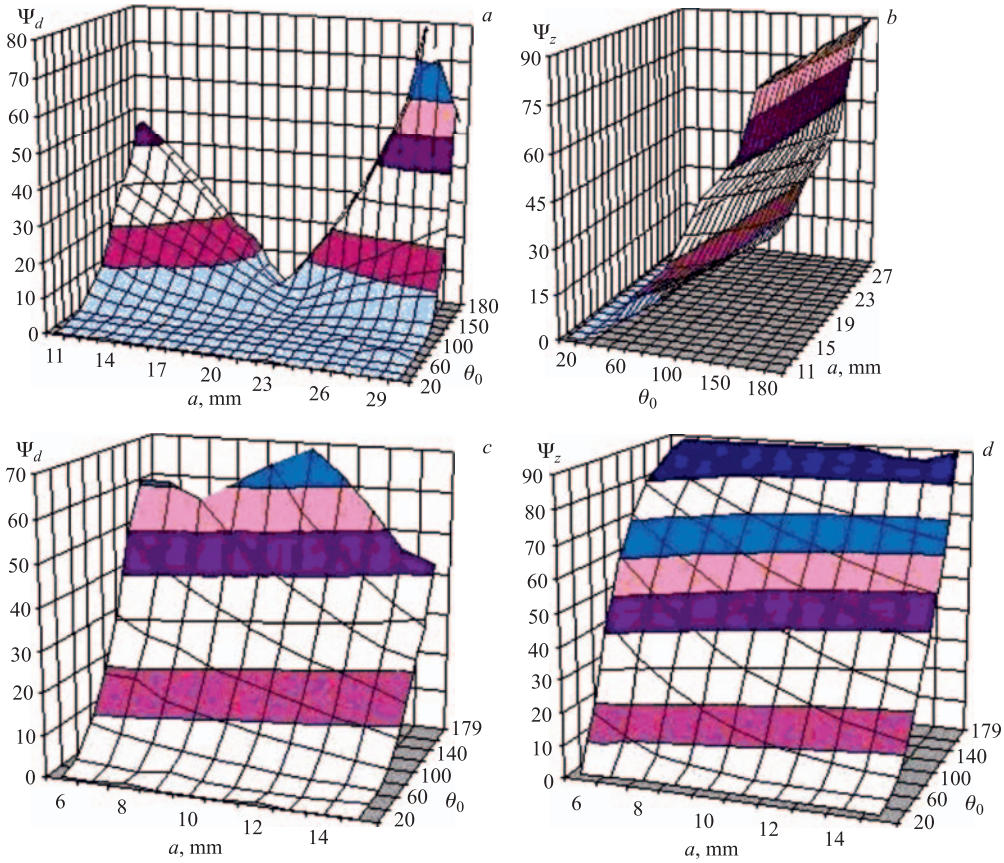

Fig. 2. Surfaces plots of $\Psi_d(a,\theta)$ (*a*, *c*), $\Psi_z(a,\theta)$ (*b*, *d*) for the DLW Fig. 1, *e* (*a*, *b*), and TE-type structure Fig. 1, *b* (*c*, *d*) [4], $\lambda = 10$ cm

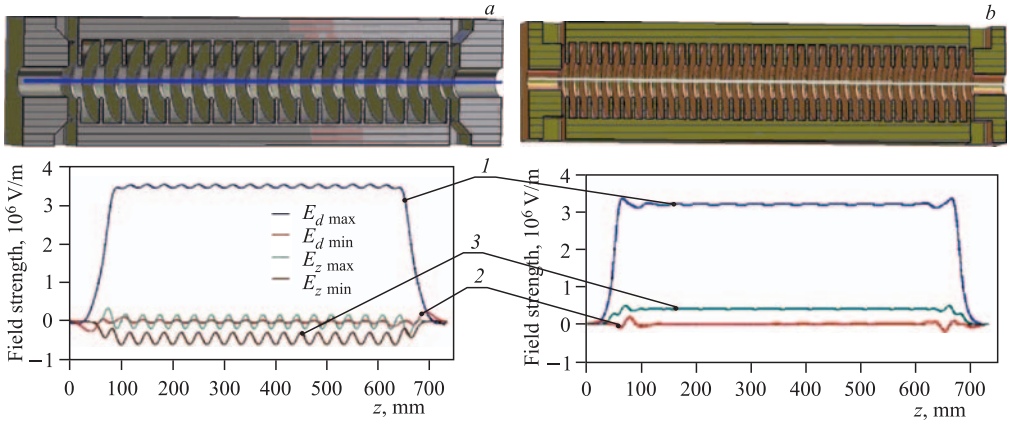

Fig. 3. Plots of E_d and E_z distributions for a DLW in the TW mode, $\theta = 120^\circ$ (*a*) and $\theta = 60^\circ$ (*b*). *1* — $E_d, \phi = 0^\circ$, *2* — $E_d, \phi = 90^\circ$, and *3* — $E_z, \phi = 90^\circ$

1.2. Standing Wave Operation. For the Standing Wave (SW) operating mode, $\theta = 180°$, the attenuation of harmonics (3) is not effective and the opposite phasing of the hybrid waves HE_1 and HM_1 together with balancing $A \sim -B$ becomes the only way for the reduction of aberrations, which turns out to be even more important than for the TW case. Even considering only the main harmonics $p = 0$ in the E_x and H_y field components, for the main E_d harmonic one finds

$$E_{dx}(z) = \frac{e_{x0} - Z_0 h_{y0}}{2} \cos(\phi) + \frac{e_{x0} + Z_0 h_{y0}}{2} \cos(2kz + \phi). \tag{5}$$

For any initial phase shift ϕ the central particle in the bunch sees both a uniform and an oscillating impact of the deflecting field. Even if the main harmonic is free from aberrations, the oscillating part in (5) shifts a bunch of particles as a whole from the DS axis to regions with higher field nonlinearities due to the higher spatial harmonics.

The study was concentrated on DS with the opposite phasing of hybrid waves — the classical DLW, and the decoupled structure, Fig. 4, *b* [2]. For the simple SW DLW, Fig. 4, *a*, the reduction of higher harmonics (2) is achieved by enlarging the iris aperture $a \sim 20$ mm, to minimize Ψ_d, Fig. 5, *b*, and balance the electric and magnetic field components so that

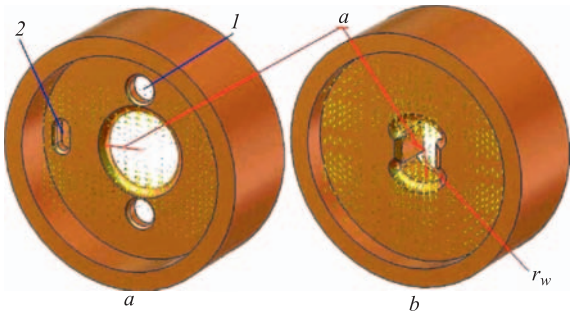

Fig. 4. The SW structures with the minimized aberrations in E_d [5]: *a*) the optimized DLW structure with holes (*1*) and slots (*2*); *b*) the decoupled structure

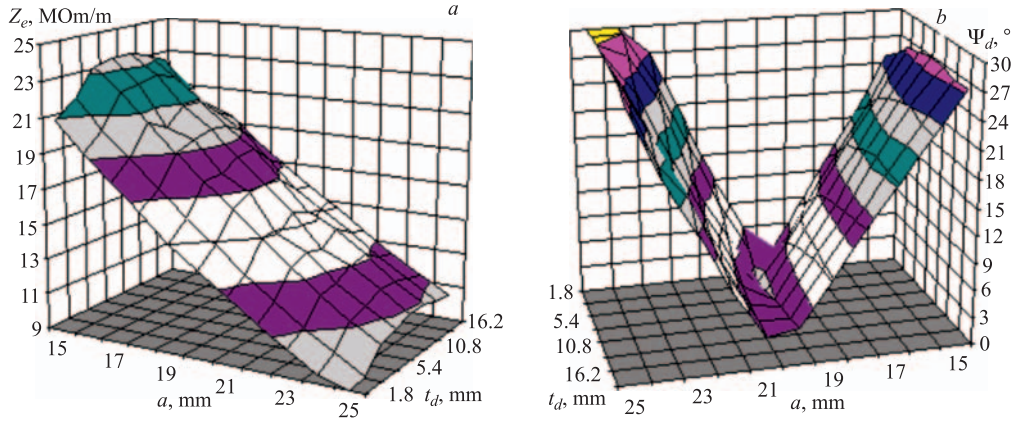

Fig. 5. The surfaces $Z_e(a, t_d)$ (*a*) and $\Psi_d(a, t_d)$ (*b*) for the SW DLW structure, $\lambda = 10$ cm

$A \sim -B$ [2]. At the same time, the effect of the oscillating term onto the average trajectory (5) is reduced. It leads, however, also to a reduction of the effective shunt impedance Z_e, Fig. 5, *a*.

Balancing the field components while keeping a high RF efficiency requires to decouple the control of the DS RF parameters for efficiency and for the field distribution near the axis, which requires structure designs with more degrees of freedom. Such a possibility was confirmed in [4] and realized in [5] by changing the parameter r_w, Fig. 4, *b*. The field distributions for the optimized DLW and two options of the decoupled structure are shown in Fig. 6.

The beam dynamics simulations through different DSs were performed with the program ASTRA, a detailed description is presented in [6]. In the Table, the most distinctive cases of the induced growth of the normalized emittance in different SW DSs for 50 MeV electron energy with an rms beam size of 1 mm, and assuming a deflecting voltage of 1 MV, $\phi = 90°$, are presented. Within the precision of the simulations no emittance growth is

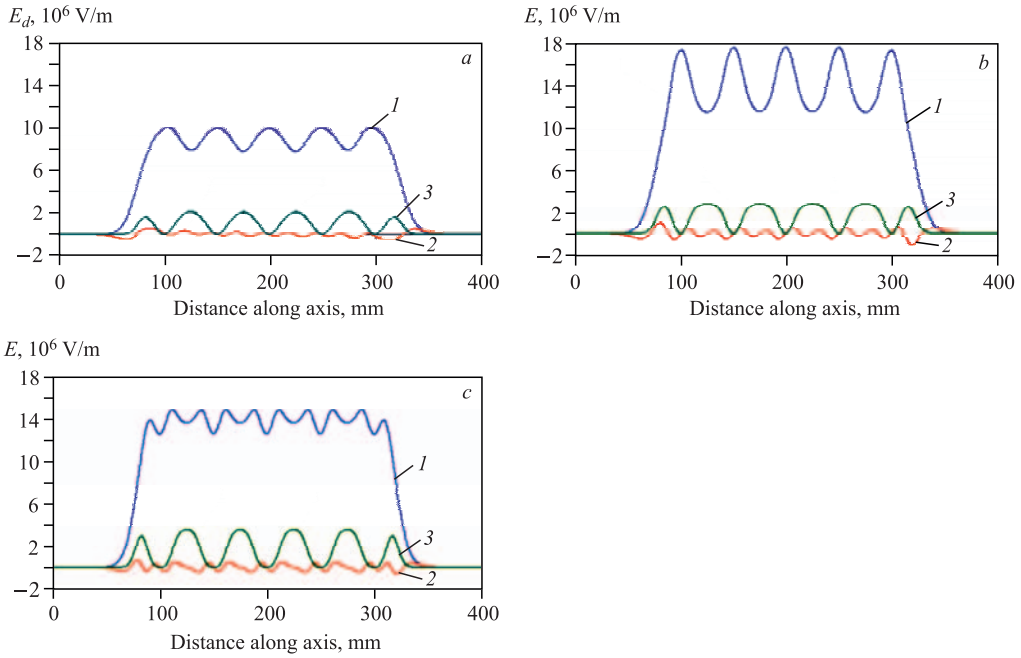

Fig. 6. The field distributions along the SW deflector axis for the optimized DLW (*a*) and two options of the decoupled structure (*b*, *c*). *1* — E_d, $\phi = 0°$; *2* — E_d, $\phi = 90°$; *3* — E_z, $\phi = 90°$

Comparison of induced emittance growth in SW DSs, $\lambda = 10$ cm

DS	a, mm	B/A	Ψ_d, °	Z_e, MOm/m	$\varepsilon_{n,x}^{\text{non}}$, 10^{-8} m
TE	6.72	0.31	180	61.0	8.1
DLW	12	–2.05	> 30	26.4	2.0
DLW	20.17	–0.86	2.39	15.9	0.0
Dec.	10.2	–0.79	2.07	36.9	0.0

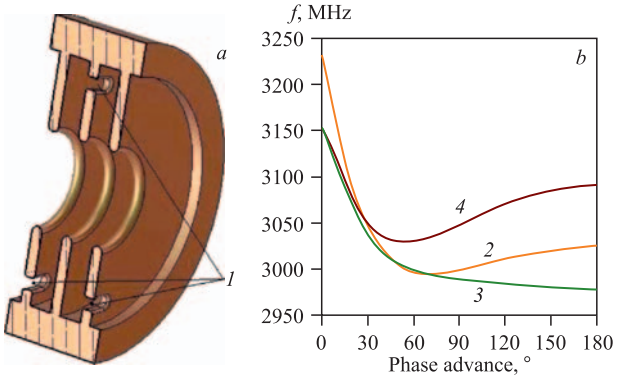

Fig. 7. The DLW DS with slots (*1*) (*a*), and dispersion curves, original (*2*), for deflecting (*3*) and for perpendicular (*4*) field polarizations after correction (*b*)

observed for the optimized SW DSs in contrast to the most effective TE structure with equal phasing of the hybrid waves and DLW $a = 12$ mm and unbalanced amplitudes of the hybrid waves. It confirms the necessity of both the reduction of oscillations (5) and higher spatial harmonics (2) for the minimization of aberrations.

2. DISPERSION CURVE CORRECTION

The opposite phasing of the hybrid waves HE_1 and HM_1 defines a negative dispersion of DS. For an effective aberration reduction the amplitudes should be balanced, $A \sim -B$, but this balance can be obtained only in the vicinity of the inversion point with $\beta_g = 0$ [2], where β_g is the group velocity of the operating wave. Differing from the predictions of the small-pitch approximation, for the real DLW the aperture radius a, for which inversion appears, depends on θ. This provides some limitations on the choice of the DS parameters. To improve the deteriorated dispersion curve, we apply the resonant method [5]. One resonant slot (*1* in Fig. 7, *a*) is introduced into the disk to interact with the modes of the operating direction. To provide a larger frequency shift with smaller slot excitation to minimize the perturbations of the optimized field distributions in DS, the slots in adjacent disks are rotated by 180°.

In Fig. 7, *b*, the influence of the slots is illustrated for the DLW TW case $\theta = 60°$, $\beta_g = -0.01$. The slot opening angle is $\sim 32°$. Such a slot opening results in a monotonous dispersion curve for the modes in the deflecting direction. Simultaneously a frequency separation with the dispersion curve for the modes with perpendicular field direction is obtained.

This work is supported in part by the RBFR grant N12-02-00654-a.

REFERENCES

1. *Hahn H.* Deflecting Mode in Circular Iris-Loaded Waveguides // Rev. Sci. Instr. 1963. V. 34, No. 10. P. 1094;
Gerault Y. Etude d'une Classe d'Ondes Electromatiques Guides: Les Ondes EH. CERN 64-33. 1964.

2. *Paramonov V.* Deflecting Structures with Minimized Level of Aberrations // Proc. of Linac 2012. Tel Aviv, 2012. P. 445; Field Distribution Analysis in Deflecting Structures. DESY 18-13. arXiv:1302.5306v1. 2013.
3. *Altenmueller O. H., Larsen R. R., Loew G. A.* Investigations of Traveling-Wave Separators for the Stanford Two-Mile Accelerator // Rev. Sci. Instr. 1964. V. 35, No. 4.
4. *Paramonov V., Kravchuk L., Floettmann K.* Parameters of a TE-Type Deflecting Structure for the S-Band Frequency Range // Proc. of Linac 2012. Tel Aviv, 2012. P. 366.
5. *Paramonov V. et al.* Standing Wave RF Deflectors with Reduced Aberrations // Proc. of RuPAC 2012. P. 590.
6. *Floettmann K., Paramonov V.* Beam Dynamics in Transverse Deflecting RF Structures // Phys. Rev. ST Accel. Beams. 2014. V. 17. P. 024001.